



Performance investigation of microphotonic-silicon devices in a field-trial all-optical network

J.D. Marconi^{a,*}, Arismar Cerqueira S. Jr.^b, J.T. Robinson^c, N. Sherwood-Droz^c, Y. Okawachi^d, H.E. Hernandez-Figueroa^b, M. Lipson^c, A.L. Gaeta^d, H.L. Fragnito^a

^a Optics and Photonics Research Center, Unicamp – IFGW, Campinas, SP 13083-970, Brazil

^b Optics and Photonics Research Center, Unicamp – School of Electrical and Computer Engineering, Campinas, SP 13083-970, Brazil

^c Electrical and Computer Engineering Department, Cornell University, Ithaca, NY 14853, USA

^d School of Applied and Engineering Physics, Cornell University, Ithaca, NY 14853, USA

ARTICLE INFO

Article history:

Received 16 September 2008

Received in revised form 6 November 2008

Accepted 7 November 2008

Keywords:

Silicon ring resonators
Silicon waveguides
Integrated optics
All-optical networks
Field-trial tests

ABSTRACT

The performance of microphotonic-silicon devices in a geographically-distributed optical fiber network is experimentally investigated. Two different devices are tested: an optical filter based on a silicon ring resonator and an all-optical wavelength converter based on four-wave mixing in a dispersion-tailored highly nonlinear silicon waveguide. The evaluation of the devices is performed by means of eye diagrams and measurements of the bit error rate.

© 2008 Elsevier B.V. All rights reserved.

1. Introduction

The predicted increase in the demand for internet bandwidth [1] has motivated the research for all-optical devices in order to improve the capacity of the present networks. It is well known that devices such as broadband optical amplifiers, all-optical wavelength converters (AOWCs) or all-optical regenerators (AORs) located at the network nodes will be indispensable for future all-optical networks.

Broadband AOWCs and AORs based on cross-gain modulation and four-wave mixing (FWM) in semiconductor optical amplifiers (SOAs) have been demonstrated [2–4]. Optical amplifiers with broad bandwidths, AOWCs, and AORs based on FWM in optical fibers were also widely studied [5–15]. Periodically poled lithium niobate (PPLN) waveguides have also been used to obtain AOWCs [16,17].

Recently, the development of high-speed silicon microphotonic and nanophotonic devices operating at telecommunication wavelengths has brought forth the exciting prospect of using chip-scale silicon-based components in optical fiber networks.

As a result of the benefits of miniaturization and integration afforded by the maturity of the silicon fabrication processes a

reduction in size, weight, power consumption and cost would be possible by using micron-sized silicon photonic devices.

Moreover, several devices may be integrated on the same silicon platform as present technology permits for monolithic, electrically controlled, chip-scale photonic devices.

An additional benefit of silicon-based optical components is that compared to silica fibers, the third-order nonlinear coefficient is $\sim 10^5$ times larger. As a consequence, devices such as AOWCs and AORs, based on FWM, could be integrated in compact chips reducing the size of the devices and therefore occupying less equipment storage space at the node centers.

Several silicon-based devices such as high-speed electro-optical modulators [18,19], switches [20,21], filters [22,23], lasers [24], optical amplifiers [25–28], AOWCs [29–31] and AORs [32,33] have been demonstrated in laboratory settings.

Despite the significant progress made in developing these photonic devices little work has been done investigating the feasibility of implementing them in real optical fiber networks. Before these devices can be commercialized it is imperative to analyze their performance under realistic conditions. Actual geographically-distributed fiber optic networks can introduce challenges for the operation of silicon photonic devices including polarization rotation and chromatic dispersion. However, access to fiber optical networks for research is limited. Therefore, the majority of the tests on

* Corresponding author. Tel.: +55 19 35215451; fax: +55 19 35215428.

E-mail address: dmarconi@ifi.unicamp.com (J.D. Marconi).

silicon photonic devices have been performed under laboratory conditions on fiber spools.

In this paper, we study the performance of two different devices in a field-trial network (Kyatera network) located in São Paulo State, Brazil [34]. The devices under test were a filter based on a microring resonator and an AOWC performed with a dispersion-tailored silicon micro-waveguide as a nonlinear medium. This field test allows us to evaluate the performance of silicon photonic devices performing linear and nonlinear operations under real working conditions.

Besides this introductory section, this paper is arranged into three additional sections. In Section 2, we present the experimental setups used to evaluate the different silicon-based devices. In Section 3, we present our experimental results for the filter and the AOWC. Finally, in Section 4, we present our conclusions.

2. Experimental setup

The experimental setup used to evaluate the microring add-drop filter is shown in Fig. 1a. The light sources were two external cavity lasers (ECL). They were externally modulated with a non-return-to-zero (NRZ) pseudo-random bit sequence (PRBS, $2^{15} - 1$) at 10 Gb/s with a lithium-niobate-based electro-optic intensity modulator (IM). These signals were then amplified with an erbium doped fiber amplifier (EDFA) and sent through a 40 km path of laid fiber in the Kyatera network.

This optical link is formed by 22.4 km (~56%) of aerial cables and 17.6 km of underground cables. All the fibers that compose this link are single mode standard fibers. To compensate for the added dispersion in the Kyatera network we included a section of dispersion compensating (DC) fiber. We have also included a dy-

namic polarization controller (DPC, Adaptif model A3300), which allowed us to fix (with the device turned on) the polarization of a randomly polarized input. The insertion loss of the DPC was <4 dB and the state of polarization accuracy was $\leq \pm 1^\circ$ in the Poincaré sphere. By switching the DPC between the on and off states, we can investigate the effect of polarization randomization on the performance of the silicon device. That randomization in the polarization state of the signal after the link is fundamentally due to the aerial cables in the network.

Using an inline static polarization controller (PC) we can then selectively excite the quasi-TM mode of the silicon waveguide. The light is then collected from the drop port of the microring filter. The total loss between the fiber input and the fiber at the microring output was ~8 dB. This could be improved by using tapered fibers. With a variable optical attenuator (VOA) we control the amount of signal reaching the receiver for bit error rate (BER) characterization. The power was monitored with an optical power meter (PM). The receiver consists of an EDFA, a band pass filter (BPF, ~ 1 nm linewidth), a BER analyzer and an oscilloscope (OSC) to record the eye diagrams. The optical spectra were measured with an optical spectrum analyzer (OSA) with 0.1 nm resolution.

A silicon microring add-drop filter, like the one tested in our experiment, is shown in Fig. 1b prior to being cladded with silicon oxide. The device was fabricated using electron beam lithography and reactive ion etching and cladded with silicon oxide using plasma enhanced chemical vapor deposition. Details of the fabrication process can be found in [35]. The radius of the ring used in our experiment is approximately 10 microns and the waveguide dimensions are 250 tall by 450 nm wide. The free spectral range of the microrings is ~8.5 nm. When the resonance condition is met (the optical path length around the ring is an integer number

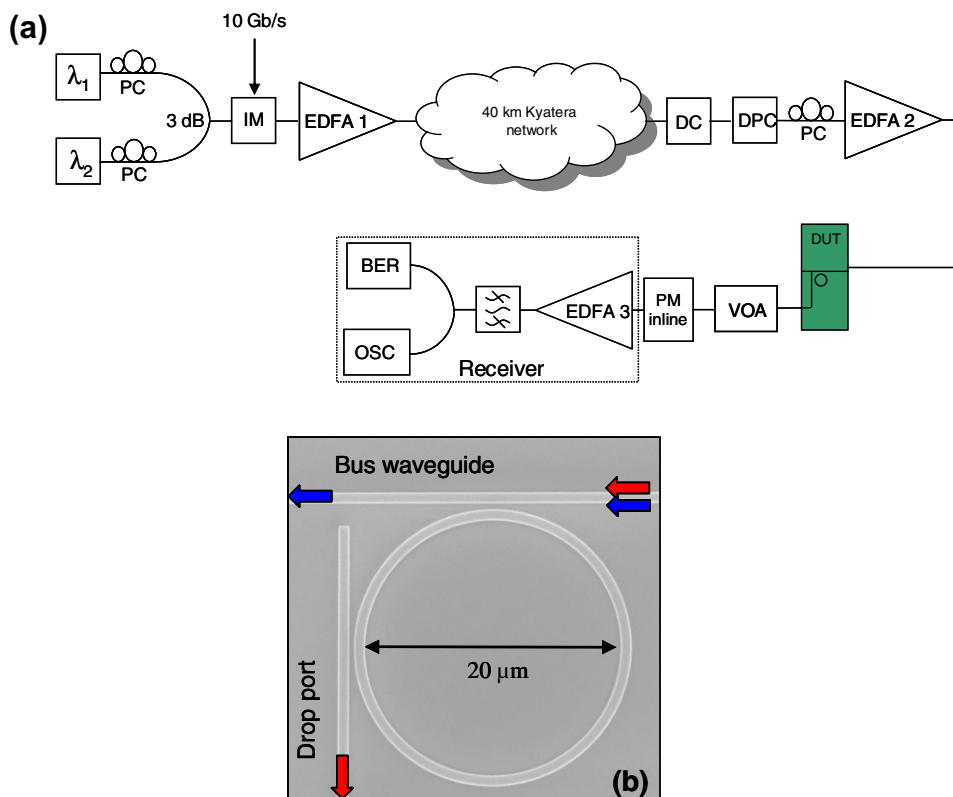


Fig. 1. (a) Experimental setup used to characterize the microring add-drop filter. (b) Scanning electron micrograph of a microring add-drop filter like the one used in our experiment. Red and blue arrows indicate the path of light for wavelengths which turn the resonance on and off, respectively. (For interpretation of the references to colour in this figure legend, the reader is referred to the web version of this article.)

of wavelengths) destructive interference between the light in the ring and the light remaining in the bus waveguide causes the light to be directed to the drop port (see Fig. 1b). A temperature controller connected to a heater located below the chip was used to tune the resonance wavelength between the two wavelengths of the ECLs.

Fig. 2 shows the experimental setup used to measure the AOWC. The ECL sources, modulation format, OSA, and OSC are all the same as the previous setup.

The signal at λ_3 is modulated with the PRBS and travels through the network, while the wave at λ_4 is a cw laser. The signal at λ_3 is amplified by EDFA 3 and used as a pump in the FWM process.

At the waveguide input we added a polarizer in order to excite the quasi-TM mode of the waves at both wavelengths. In the receiver we used the same model EDFA pre-amplifier. BPF1 has the same characteristics than the BPF2 and is used to filter the converted signal.

In this experiment, we used an optical network link with a 20 km length with the same percentages of aerial and underground cables as the previous experiment. The dispersion compensator was not used in this case due to power limitations. The insertion loss of the DC device was ~ 11 dB. Such loss results in insufficient

power at the input of EDFA 3 to generate enough power to achieve FWM in the silicon waveguide. However, since the link used here was only 20 km in length, the dispersion-induced distortion in the eye diagram was tolerable.

The dimensions of the waveguide used in this experiment were carefully chosen (300 nm tall and 500 nm wide) such that the modal and material dispersion canceled creating zero group velocity dispersion [36]. This allows us to achieve highly efficient FWM due to the phase matching of the signal and generated waves. The waveguide used here is 1.8 cm in length.

3. Experimental results and discussion

In order to study the performance of our silicon waveguides working as linear devices, we used the ring resonators as a filter, according to the setup in Fig. 1a. First, two signals at $\lambda_1 = 1555.12$ nm and $\lambda_2 = 1559.42$ nm were launched through the Kyatara network. The resonance wavelength of the ring used to select the desired wavelength was tuned by using a temperature controller. This allowed us to use the microring as a tunable filter, enabling us to select either, the channel at λ_1 or the channel at λ_2 . Since the extinction ratio of the rings is ~ 15 dB, the signal at

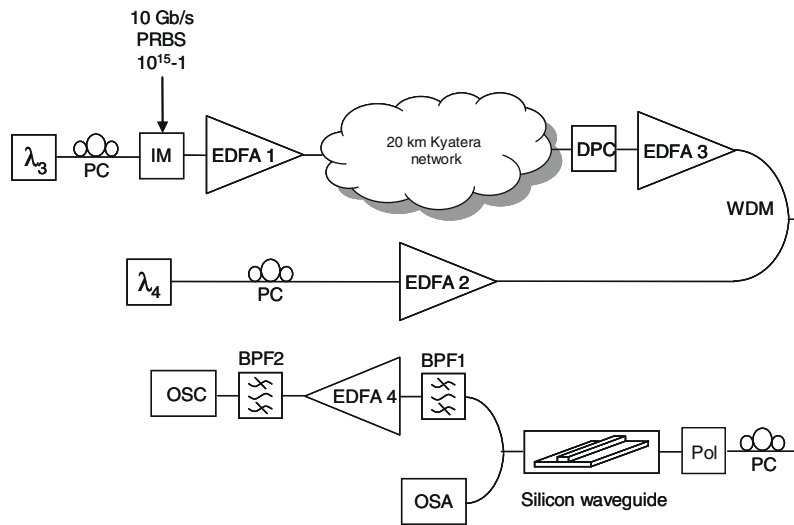


Fig. 2. Experimental setup of the AOWC experiment.

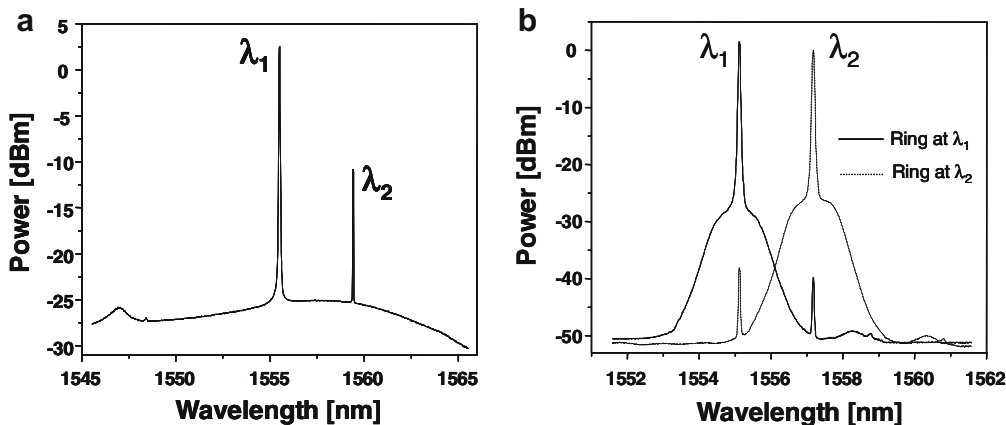


Fig. 3. (a) Output spectra at the output of the EDFA3. The difference between the powers at λ_1 and λ_2 is ~ 14 dB. (b) Output after the BPF of the receiver. The continuous line shows the spectrum when the ring is tuned to λ_1 , meanwhile the dotted line shows the spectrum when the ring is tuned to λ_2 . The tuning was achieved using a temperature controller located below the microring.

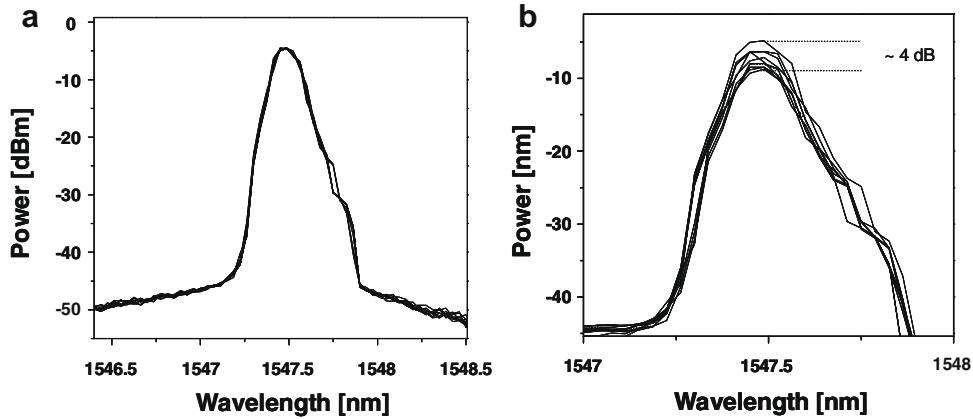


Fig. 4. Spectra at the output of the microring. (a) With the DPC turned on. (b) With the DPC turned off.

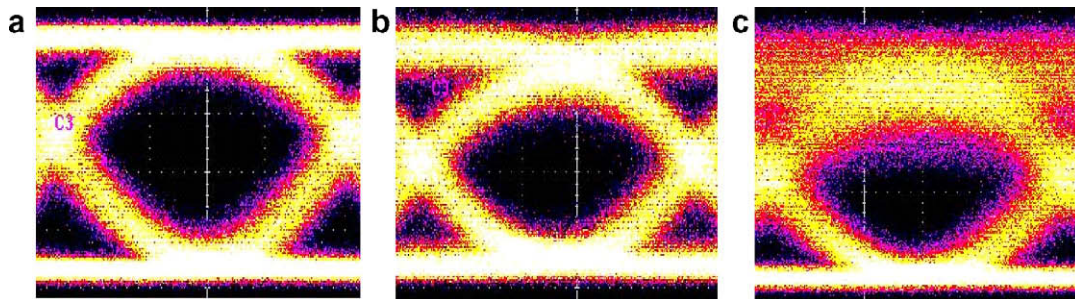


Fig. 5. Eye diagrams: (a) before the input signal be launched through the Kyatera network. (b) At the ring output with the DPC turned on. (c) At the ring output with the DPC turned off.

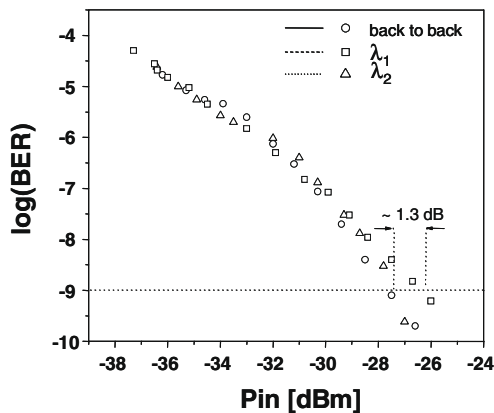


Fig. 6. BER, as a function of the input power in the receiver, for the signal passing through the microring filter.

λ_2 at the output of EDFA 3 is ~ 15 dB below the signal at λ_1 , as shown in Fig. 3a. This difference is not enough to ensure a good quality reception so it is necessary to have the band pass filter after EDFA 3. This filter is already part of the receiver, but in this case it is also necessary to avoid crosstalk between the signals. Fig. 3b shows the spectrum after the BPF. In this case we set the resonance of the microring at $\lambda_2 = 1557.18$ nm. The distance from λ_1 is approximately the shortest allowed for the bandwidth of our filter. As shown later on, the use of the microring filter does not imposed appreciable penalty to the modulated signal.

The rectangular geometry of waveguides used in our experiment produces a birefringence between the quasi-TE and quasi-TM

modes. As a consequence, the resonance wavelength and quality factor of the microring will be different for the two polarizations. The difference between the resonance wavelengths of the quasi-TM and the quasi-TE modes is ~ 1 nm (the high wavelength corresponds to the quasi-TE mode). The bandwidth at -3 dB of the quasi-TM mode was ~ 1 nm and it was ~ 0.1 nm for the quasi-TE mode, producing a Q factor ~ 10 -fold higher than that of the quasi-TM case.

Since the wavelengths used in this experiment are on resonance for the quasi-TM fundamental mode, a fluctuating polarization will imply in a variation of the input light between on and off resonance conditions. As it was previously mentioned, the link used to evaluate our devices has ~ 23 km of aerial cables, which induce strong random variation in the polarization of light propagating through the network (for further details see Appendix A, which presents some polarization measurements). To evaluate the impact of these fluctuations in the microring filter we record a set of 10 successive spectra at ~ 20 s intervals at the ring output with and without the DPC (in this case we used a microring with a resonance wavelength of 1547.5 nm, different from the one used previously). The results are shown in Fig. 4. It is easy to see that there is no power fluctuation when the DPC is turned on, while a variation of 4 dB appears when it is turned off.

The effect of the random induced polarization changes can also be observed from the eye diagrams of the modulated signal at the output of the BPF in the receiver. Fig. 5a shows the eye diagrams at the input of the device, and Fig. 5b and c at the output of the microring with the DPC turned on and off, respectively. In all cases we show a 10 s time averaged eye diagram. We see that by incorporating the DPC we could recover an eye diagram with a significantly better quality factor in comparison with the case with the DPC

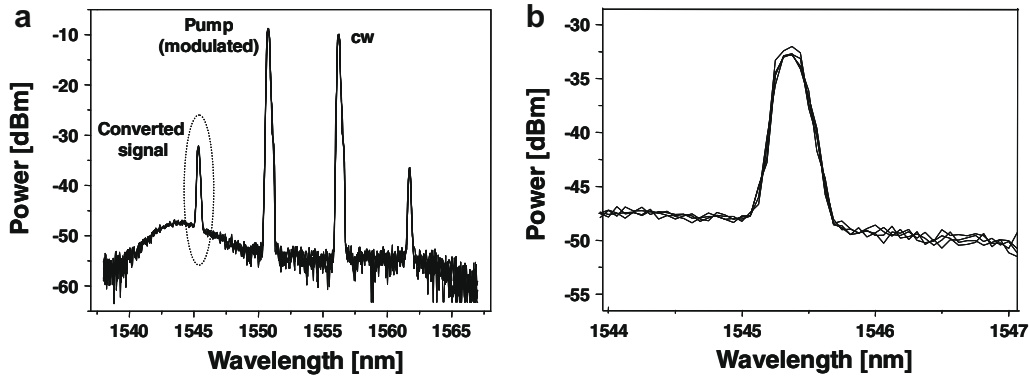


Fig. 7. Output spectra with the DPC turned on. (a) Complete spectra; (b) zoom of the converted signal.

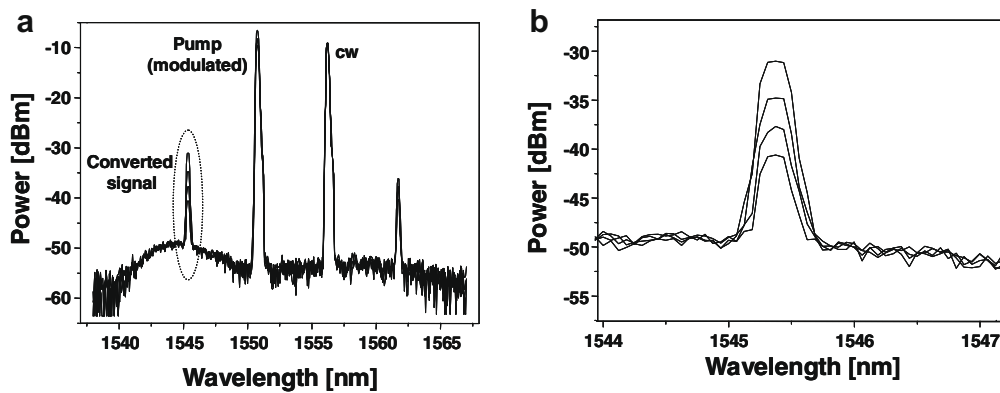


Fig. 8. Output spectra with the DPC turned off. (a) Complete spectra; (b) zoom of the converted signal.

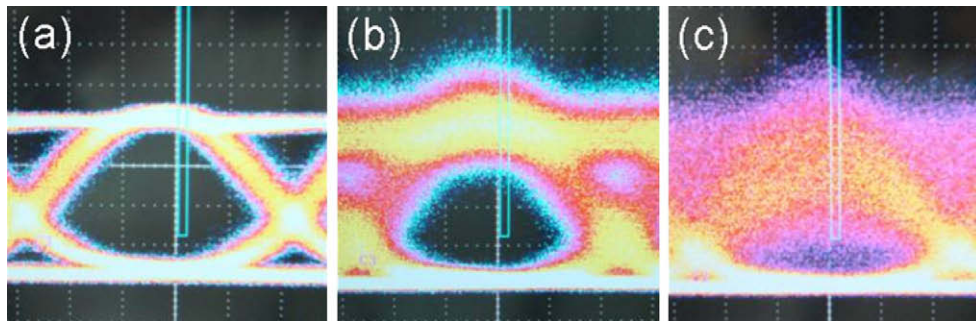


Fig. 9. Eye diagrams. (a) Input of the silicon waveguide. (b) Output with the DPC turned on. (c) Output with the DPC turned off.

turned off. Indeed when the DPC is off, we observed the eye diagram fluctuating between open and closed states in a minute's time. This fluctuation prevents us from measuring a meaningful BER.

All these results show that in order to overcome this fluctuating polarization rotation produced by the geographically-distributed optical network, a DPC or similar method must be used to stabilize the polarization. The polarization diversity technique is an interesting alternative for obtaining transparent polarization devices. It was proposed for parametric amplifiers in [37] and it has been demonstrated for silicon waveguides in [38,39].

Finally in Fig. 6 we present the BER as a function of the input power at the input of the BER analyzer, obtained while using the DPC. The signals were modulated with a pseudo-random bit sequence (PRBS, $2^{15}-1$).

We controlled the power sent to the receiver using a VOA. A penalty of ~ 1.3 dB at a BER of 10^{-9} was induced for the ring with respect to the back to back measurement. The difference between the BER of the signal at channels 1 and 2 was ~ 0.5 dB, which is inside the error of our measurements. This means that the silicon microrings do not introduce a significant penalty when used as a filter and as a consequence could be used for ultra-compact multiplexers and demultiplexers for DWDM systems.

To analyze the performance of a silicon device for nonlinear operations we performed an AOWC based on the FWM process. Since in this process the power in the converted signal wavelength has a quadratic dependence with the pump power (which in our case carries the modulated information), we expect to see decreased fluctuation in the zero level in the eye diagram [33].

The FWM process is most efficient when the waves involved have parallel polarization states [37], and travel at the same phase velocity. Since phase matching in this waveguide is only achieved for the quasi-TM polarization [36], random fluctuations in the polarization induced by the network result in strong power fluctuations in the converted signal. This problem was overcome with the DPC as shown in Fig. 7, where a set of four spectra recorded over 10 s steps appear without power variation. The conversion efficiency was ~ -22 dB. To illustrate the magnitude of the variations produced on the idler power for the polarizations variations, we record another set of spectra with the DPC is turned off. The result is shown in Fig. 8 where variations in the converted signal power as high as 10 dB are observed.

The eye diagrams of the signals after the 20 km link are shown in Fig. 9a–c. In (a) we can see the eye diagram at the input of the waveguide. In (b) and (c) we have the eye diagrams of the converted signal with the DPC turned on and off, respectively. The calculated standard deviation of the zero level of the eye diagram shown in Fig. 9b had an improvement, dropping from 0.033 to 0.027. The one level appears more noisy owing to the free carriers absorption effect [33]. This problem can be resolved by electrically biasing the waveguide to sweep out the generated free carriers.

Fig. 9c shows the variations in the amplitude of the converted wave when the DPC is turned off. This clearly demonstrates the need for polarization control in maintaining open eye diagrams for the FWM process.

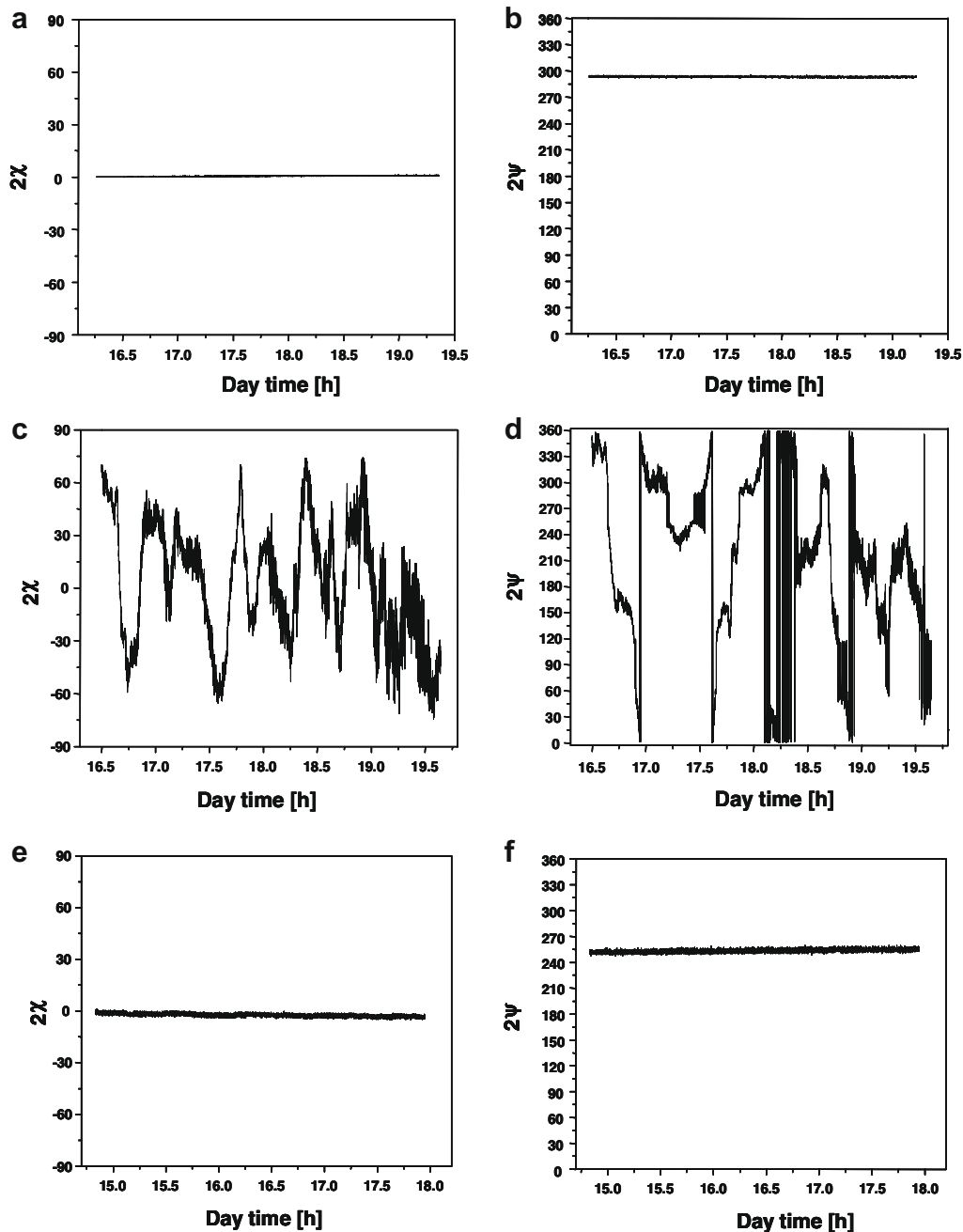


Fig. A1. Polarization measurements along three hours for: (a) and (b). The signal laser directly connected to the polarimeter. (c) and (d). The signal laser after passing through the Kyatera network with the DPC turned off. (e) and (f). The laser after passing through the Kyatera network with the DPC turned on.

4. Conclusions

We have evaluated the performance of an optical filter based on a silicon microring and an AOWC based on a silicon waveguide in a field-trial optical network.

In both devices the response was strongly affected by the random polarization variations of the signal. This happened after the signal traveled through the fiber link. A technique based on a dynamic polarization controller was able to overcome this limitation.

For the filter, the power penalty was only ~ 1.3 dB in relation to the back-to-back case. This low power penalty may allow the cascading of several microring resonators to obtain ultra-compact DWDM multiplexers-demultiplexers. Also, tunable optical filters using temperature as the control parameter could be used as practical devices.

In the AOWC case, the zero level of the converted wave eye diagram was improved. The calculated standard deviation dropped from 0.033 to 0.027.

In summary, we have shown that once the polarization fluctuations have been compensated, both linear and nonlinear functions can be performed using silicon microphotonic devices in real geographically-distributed fiber networks.

Acknowledgements

The authors thank Amy C. Turner and Mark A. Foster from the School of Applied and Engineering Physics (Cornell University, USA) for the fabrication of the silicon waveguides used in the wavelength conversion experiments. The authors from Brazil thank the Brazilian agencies FAPESP (Contracts: 2006/52952-1 (A. Cerqueira's Postdoctoral fellowship), 2006/50911-6 (J.D. Marconi's Postdoctoral fellowship) and 2005/51689-2 (CePOF)), CAPES and CNPq (Contract: 305992/2005-8) for their financial support.

Appendix A

Fig. A1 shows the polarization measurements to illustrate the strong variations induced in a real network with aerial cables. The presented angles 2χ and 2ψ are the ones referred to the Poincaré sphere according to the formalism presented in Ref. [40]. The polarization measurements were made during one entire day in intervals of three hours. In the set shown in Fig. A1 we present the measurements between $\sim 4:00$ pm and $7:00$ pm. Fig. A1a and b show the measurements of the signal laser directly without passing through the Kyatera network. Fig. A1c and d show the signal laser after it has passed through the network with the DPC turned off. Finally, Fig. A1e and f show the laser after passing through the Kyatera network with the DPC turned on.

It is clear how the DPC is able to stabilize the polarization at the output even with the strong variations present at the input.

References

- [1] E.B. Desurvire, *J. Lightwave Technol.* 24 (2006) 4697.
- [2] Y. Hong, P.S. Spencer, K.A. Shore, *IEEE J. Quantum. Electron.* 40 (2004) 152.
- [3] M. Matsuura, N. Kishi, T. Miki, *J. Lightwave. Technol.* 25 (2007) 38.
- [4] C. Bornholdt, J. Slovak, B. Sartorius, *Electron. Lett.* 40 (2005) 192.
- [5] G. Contestabile, R. Proietti, N. Calabretta, E. Ciaramella, *Photon. Technol. Lett.* 17 (2005) 2523.
- [6] T. Akiyama, M. Ekawa, M. Sugawara, K. Kawaguchi, H. Sudo, A. Kuramata, H. Ebe, Y. Arakawa, *Photon. Technol. Lett.* 17 (2005) 1614.
- [7] K. Inoue, H. Toba, *Photon. Technol. Lett.* 4 (1992) 69.
- [8] M. Westlund, J. Hansryd, P.A. Andrekson, S.N. Knudsen, *Electron. Lett.* 38 (2002) 85.
- [9] J.D. Marconi, J.M.C. Boggio, H.L. Fragnito, in: *Proceedings of the European Conference on Optical Communications, ECOC 2005, Paper Mo4.5.6, Glasgow, Scotland, UK, 2005.*
- [10] J. Jiang, R. Saperstein, N. Alic, M. Nezhad, C. McKinstrie, J. Ford, Y. Fainman, S. Radic, *Photon. Technol. Lett.* 18 (2006) 2445.
- [11] K. Inoue, *Electron. Lett.* 36 (2000) 1016.
- [12] K. Inoue, *Photon. Technol. Lett.* 13 (2001) 338.
- [13] J.M.C. Boggio, J.D. Marconi, S.R. Bickham, H.L. Fragnito, *Opt. Express* 15 (2005) 5288.
- [14] S. Radic, C.J. McKinstrie, *IECE Trans. Electron.* E88 (2005) 859.
- [15] T. Torounidis, P.A. Andrekson, B.E. Olsson, *Photon. Technol. Lett.* 18 (2006) 1194.
- [16] M.H. Chou, K.R. Parameswaran, M.M. Fejer, *Opt. Lett.* 24 (1999) 1157.
- [17] H. Furukawa, A. Nirmalathas, N. Wada, S. Shinada, H. Tsuboya, T. Miyazaki, *Photon. Technol. Lett.* 19 (2007) 384.
- [18] L. Liao, D. Samara-Rubio, M. Morse, A. Liu, D. Hodge, D. Rubin, *Opt. Express* 13 (2005) 3129.
- [19] Q. Xu, B. Schmidt, S. Pradhan, M. Lipson, *Nature* 435 (2005) 325.
- [20] P. Dong, S.F. Preble, M. Lipson, *Opt. Express* 15 (2007) 9600.
- [21] D.M. Beggs, T.P. White, L. O'Faolain, T.F. Krauss, *Opt. Lett.* 33 (2008) 147.
- [22] F. Xia, M. Rooks, L. Sekaric, Y. Vlasov, *Opt. Express* 15 (2007) 11934.
- [23] A. Melloni, M. Martinelli, G. Cusmai, R. Siano, *Opt. Commun.* 234 (2004) 211.
- [24] H. Rong, R. Jones, A. Liu, O. Cohen, D. Hak, A. Fang, M. Paniccia, *Nature* 433 (2005) 725.
- [25] R. Claps, D. Dimitropoulos, V. Raghunathan, Y. Han, B. Jalali, *Opt. Express* 11 (2003) 1731.
- [26] R.L. Espinola, J.I. Dadap, R.M. Osgood Jr., S.J. McNab, Y.A. Vlasov, *Opt. Express* 12 (2004) 3713.
- [27] V. Raghunathan, D. Borlaug, R.R. Rice, B. Jalali, *Opt. Express* 15 (2007) 14355.
- [28] M.A. Foster, A.C. Turner, J.E. Sharping, B.S. Schmidt, M. Lipson, A.L. Gaeta, *Nature* 441 (2006) 960.
- [29] H. Fukuda, K. Yamada, T. Shoji, M. Takahashi, T. Tsuchizawa, T. Watanabe, J. Takahashi, S. Itabashi, *Opt. Express* 13 (2005) 4629.
- [30] Y.H. Kuo, H. Rong, V. Sih, S. Xu, M. Paniccia, *Opt. Express* 14 (2006) 11721.
- [31] M.A. Foster, A.C. Turner, R. Salem, M. Lipson, A.L. Gaeta, *Opt. Express* 15 (2007) 12949.
- [32] R. Salem, M.A. Foster, A.C. Turner, D.F. Geraghty, M. Lipson, A.L. Gaeta, *Opt. Express* 15 (2007) 7802.
- [33] R. Salem, M.A. Foster, A.C. Turner, D.F. Geraghty, M. Lipson, A.L. Gaeta, *Nature Photon.* 2 (2008) 35.
- [34] <<http://www.kyatera.fapesp.br>>.
- [35] B.G. Lee, B.A. Small, K. Bergman, Q. Xu, M. Lipson, *Opt. Lett.* 31 (2006) 2701.
- [36] A.C. Turner, C. Manolatou, B.S. Schmidt, M. Lipson, M.A. Foster, J.E. Sharping, A.L. Gaeta, *Opt. Express* 14 (2006) 4357.
- [37] K.K. Wong, M.E. Marhic, K. Uesaka, L.G. Kazovsky, *Photon. Technol. Lett.* 14 (2002) 1506.
- [38] T. Barwicz, M.R. Watts, M.A. Popovic, P.T. Rakich, L. Socci, F.X. Kartner, E.P. Ippen, H.I. Smith, *Nature Photon.* 1 (2007) 57.
- [39] H. Fukuda, K. Yamada, T. Tsuchizawa, T. Watanabe, H. Shinjima, S. Itabashi, *Opt. Express* 16 (2008) 4872.
- [40] Max Born, Emil Wolf, *Principles of Optics*, Cambridge University Press, 1999.